ADCONIP
2014
Hiroshima

Simulation and Formula Regression of an Air Separation Unit in China Steel Corporation

Ming-Lung Li, Hao-Yeh Lee, Ming-Wei Lee and I-Lung Chien

Abstract— **Air separation Units (ASU) is widely used in many industries. ASU is difficult to operate due to high degree of energy integration. In this paper, steady-state and dynamics simulation of one of China Steel Corporation's air separation unit have been studied. The goal is to figure out the formula among gaseous product demands and set points values of the control loops in this unit, and to build up the dynamic model of this air separation unit hoping to improve the operation. Regression formula fits well to the steady state model and can be used to predict the set point values when gaseous products demand changes.**

I. INTRODUCTION

AIR is mainly composed of nitrogen, oxygen and argon, and these three gases are widely used in many industries. Oxygen is used in metals production, chemicals and gasification, petroleum refineries, medical, concrete and welding industries. Nitrogen is used in the chemical, petroleum and food industries and it is also used extensively by the electronics and metals industries for its inert properties. Argon is used as an inert material in welding, steelmaking, heat treating, and in the manufacturing processes for electronics [1].

Because of the different demand for the gas purity, gas amount, and gas usage, there are two different types of air separation processes. If a lower volume, gaseous oxygen or nitrogen product is required, then non-cryogenic processes (pressure swing adsorption & membrane separation) may be used [1]. Pressure swing adsorption systems operate on the principle of adsorption and use carbon molecular sieves. Membrane systems operate based on selective permeation [2]. On the other hand, for liquid products, larger volume gaseous products, high purity products, or the recovery of argon, cryogenic air separation processes will be used [1]. Cryogenic air separation processes separate air components according to their different boiling temperatures [3].

This paper is based on one of China Steel Corporation's (CSC) air separation unit which is a cryogenic air separation process. Cryogenic air separation process, also known as air separation unit (ASU), is an energy-intensive process that consumes a tremendous amount of electrical energy [3]. Cryogenic air separation process is operated at extremely low temperatures (-170 to -195°C) and high degree of energy integration, which makes it difficult to operate [4]. Besides, in many manufacturing processes, gaseous product demand is not fixed which leads to large changes in production rate for ASU (typically 75~105%). Therefore, ASU must rapidly respond to the changing product demands. Otherwise, excess oxygen has to be released, which leads to products lost and high operating cost, so there is significant interest in reducing the operating cost of ASU through advanced process control and optimization technology. [3,4].

Today, using advanced control and optimization technology to implement automatic load change (ALC) system in the air separation industry is an urgent need, which can provide 5~10% benefits for ASU [3]. In CSC's ASU, the set point changes are manipulated by operator's experience. Hence the goal of this paper is to figure out the formula among gaseous product demands and set point values of the control loops in this unit, and to build up the dynamic model of this air separation unit hoping to improve the operation.

II. THERMODYNAMIC MODELS

There are three components in the ASU simulation, includes nitrogen, oxygen, and argon. The PENG-ROB model is selected to describe the vapor-liquid and liquid-liquid equilibria. But the product specification could not match with plant data by using Aspen plus built-in parameters. Refer to a book by Liu [5], it suggest all the binary parameters should revise. But using Liu's parameters, the Ar-O_2 parameter is too aggressive which would cause some problems in the simulation of crude argon column (CAC), so Ar-O_2 parameter is adjusted by fitting plant data. The parameters are shown in Table 1.

After using new parameters, the simulation results are much more close to the plant data. The comparison is shown in Table 2, and the values in the parenthesis are plant data.

TABLE 1 PENG-ROB BINARY PARAMETERS (KAIJ)

	N_2-Ar	N_2-O_2	Ar-O_2
Aspen	-2.6×10^{-3}	-0.0119	0.0104
Liu	-4.7×10^{-3}	-0.0124	0.0268
This Paper	-4.7×10^{-3}	-0.0124	0.0160

This work was supported by the China Steel Corporation under Grant No RE101632

Second author is with Department of Chemical Engineering, National Taiwan University of Science & Technology, Taipei 106, Taiwan. Third author is with China Steel Corporation, Kaohsiung 812, Taiwan. Other authors are with Department of Chemical Engineering, National Taiwan University, Taipei 106, Taiwan (corresponding author: I-Lung Chien, phone: 886-2-3366-3063; fax: 886-2-2362-3040; e-mail: ilungchien@ntu.edu.tw).

TABLE 2 PENG-ROB BINARY PARAMETERS (KAIJ)

Parameters	This Paper	Aspen built-in
Gaseous O_2 Purity	**99.76 %wt** (99.66%wt)	**99.54 %wt** (99.66%wt)
Gaseous O_2 Flowrate	**18241.8 Nm^3/h** (18347.1 Nm^3/h)	**16668.2 Nm^3/h** (18347.1 Nm^3/h)
Gaseous N_2 Purity	**0.352 PPM** (0.203 PPM)	**1.6 PPM** (0.203 PPM)
Gaseous N_2 Flowrate	**45674.0 Nm^3/h** (44991.8 Nm^3/h)	**47168.7 Nm^3/h** (44991.8 Nm^3/h)
Liquid O_2 Flowrate	**191.3 Nm^3/h** (280 ~ 370 Nm^3/h)	**293.7 Nm^3/h** (280 ~ 370 Nm^3/h)
Liquid N_2 Flowrate	**319.5 Nm^3/h** (322.6 Nm^3/h)	**252.2 Nm^3/h** (322.6 Nm^3/h)
Waste N_2 Flowrate	**26009.1 Nm^3/h** (25998.6 Nm^3/h)	**26130.7 Nm^3/h** (25998.6 Nm^3/h)
Crude Ar Purity	**O_2 ： 1.68 %wt** (O_2 ： 1.88 %wt) **$O_2 + N_2$ ： 2.02 %wt** ($O_2 + N_2$ ： 2.19 %wt)	**O_2 ： 1.75 %wt** (O_2 ： 1.88 %wt) **$O_2 + N_2$ ： 1.77 %wt** ($O_2 + N_2$ ： 2.19 %wt)
Crude Ar Flowrate	**564.1 Nm^3/h** (559.1 Nm^3/h)	**483.6 Nm^3/h** (559.1 Nm^3/h)
Crude Ar Feed Purity	**O_2 ： 90.3 %wt** (O_2 ： 90.5 %wt)	**O_2 ： 90.9 %wt** (O_2 ： 90.5 %wt)

III. PROCESS DESIGN AND SIMULATION

The process is based on one of the CSC's ASU. First, the air feed is compressed by a multi-stage turbo compressor with intercoolers at a supply pressure about 6 bar. Next the air feed is cooled with water in a direct contact cooler and then removal of CO2, water vapor and hydrocarbons in molecular sieve absorbers.

After purification, most of the air feed is then cooled down to nearly liquefaction by heat exchange with exiting product and waste nitrogen and sent to a set of integrated distillation columns where the air is separated into oxygen, nitrogen, and argon.

Rest of the air feed goes for further compression by an air compressor and goes through expansion to cool the air feed in an expansion turbine. The simplified flowsheet is shown in Fig. 1.

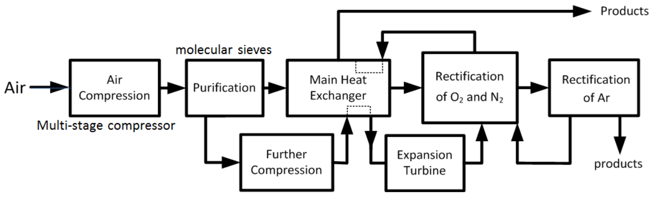

Fig. 1. Simplified flowsheet of CSC's ASU.

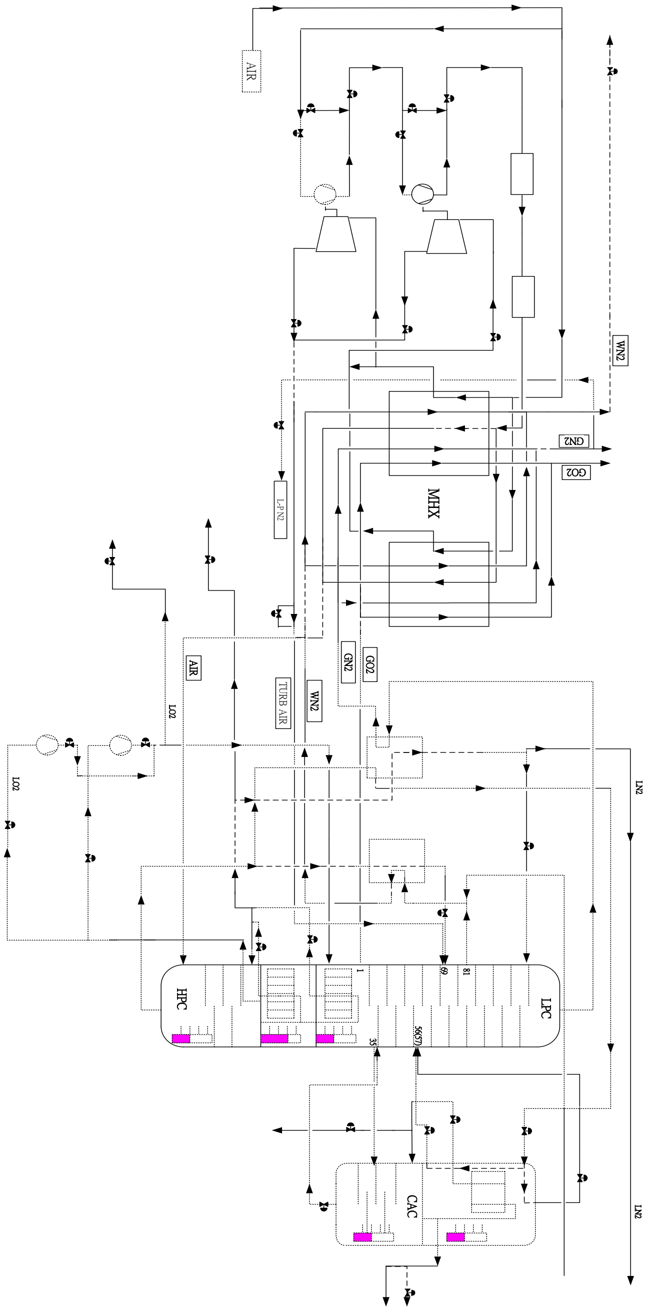

Fig. 2. The flowsheet of simulation part

Due to the uncertainty of efficiency and reaction kinetics in the final purification step for the crude argon stream by reacting oxygen with hydrogen, this paper only simulates the part after molecular sieves up to the crude argon column and does not include the final purified argon column. The flowsheet of simulation part is shown in Fig. 2.

This paper uses Aspen Plus V7.3 and Aspen Plus Dynamics as simulation tools. The Aspen flowsheet is shown in Fig. 3. The steady state simulation includes 3 parts：

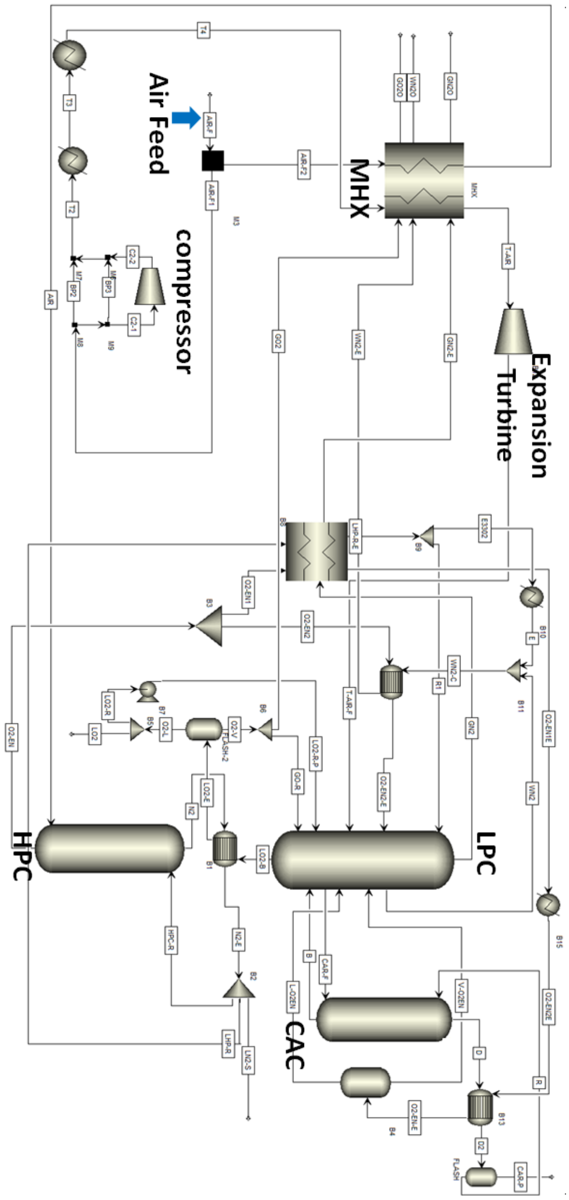

Fig. 3. The Aspen simulation flowsheet.

main heat exchanger (MHX) & compressor & turbine, high-pressure column (HPC) & low-pressure column (LPC), and crude argon column (CAC). Because the high degree of heat integration and large amount of recycles, each part is individually simulated and then combined into a complete flowsheet. The research also needs to predict or assume some values because of lacking of data in the cold box not having corresponding sensors.

In the steady-state simulation, the flowsheet maximum evaluations have to be increased from 30 to 200 and LPC's maximum iterations from 25 to 50 in order to make the flowsheet easier to converge. Some heat exchangers include vapor-liquid phase change and then separate, these heat exchangers can be replaced with a HeatX unit and a FLASH unit in simulation.

The explanation of individual part is shown as follow:

A. Main Heat Exchanger (MHX), Compressor & Turbine

At the normal conditions, only one compressor and one turbine are used. The pressure of the compressed air is about 9 bar and the two coolers use cooling water to cool down the compressed air. The MHX is composed of eight heat exchanges in the real plant, but the air split fractions are unknown, so it's hard to simulate the real configuration. The solution is to use one multi-stream heat exchanger (MHEATX) to represent the eight heat exchangers because of the similar exits' condition. After going through the turbine, the pressure of the compressed air is about 1~2 bar. All the differences can be found in Fig. 2. and Fig. 3.

The ratio between turbine air and air feed is in the range of 13~16%. Adjust this ratio can produce different amount of liquefied products.

B. High-Pressure Column (HPC)

The configuration of HPC is shown in Fig. 4. The air feed (no further compression) is cooled down to nearly liquefaction by MHX and sent to the bottom tray of the HPC. The bottom outlet stream (O2-EN) of HPC is called rich liquid (RL) [6] which contains about 30~40 wt% oxygen. RL exchanges heat with waste nitrogen and gaseous nitrogen and then goes to the low-pressure column (LPC) as feed. The condenser-reboiler is the heat exchange between HPC and HPC, and it condenses nitrogen in the top of HPC. It is assumed that N2-E stream vapor fraction = 0 for lack of temperature data. The N2-E stream serves as the reflux for both HPC and LPC. Due to lack of Fsplit's (B2) data, this split fraction is changed to vary the mass flow rate of reflux ratio in order to match the product flow rates and product purities. The result shows that split fraction of HPC-R is 0.61. LN2-S is liquid nitrogen product, and this split fraction is about 0.0038.

C. Low-Pressure Column (LPC)

The configuration of LPC is shown in Fig. 5. The

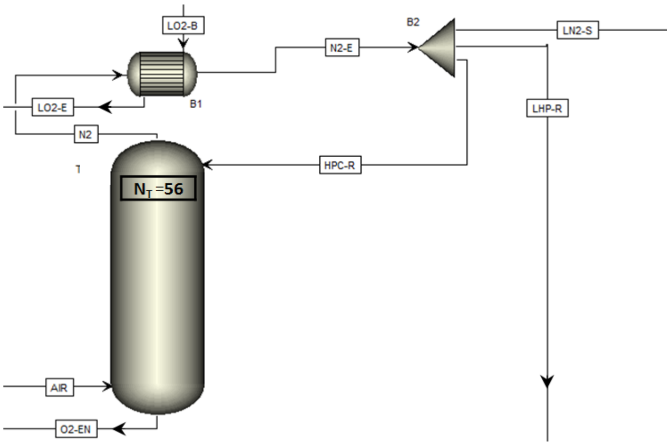

Fig. 4. The configuration of HPC

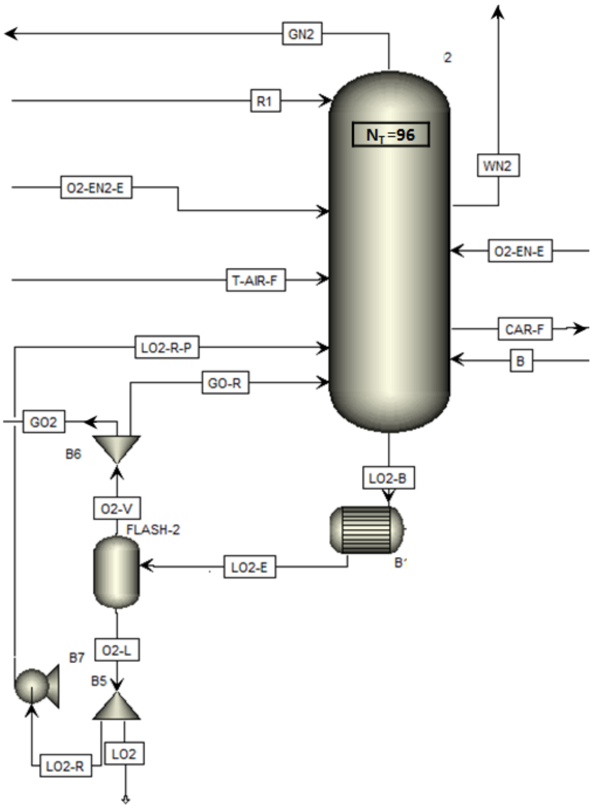

Fig. 5. The configuration of LPC

gaseous oxygen product (GO2) comes from LPC's bottom tray, and it is separated into partial liquid (LO2) and partial vapor (GO2) by condenser-reboiler. Purity and flow rate of gas oxygen product can be controlled by changing the Fsplit's (B6) split fraction, but it will also influence the purity of crude argon feed (CAR-F). Flow rate of liquid oxygen product (LO2) can be controlled by changing the reflux (R1) which comes from the top of HPC. The purpose for FLASH-2 is to separate the gas oxygen and liquid oxygen, so FLASH-2 is set at the same pressure as LO2-E and heat duty = 0. The oxygen concentration of crude argon feed (CAR-F) is important for controlling the purity of crude argon. The gaseous nitrogen product (GN2) comes from the top of LPC. This ASU uses the waste nitrogen (WN2) to increase the purities of gaseous oxygen product (GO2) and gaseous nitrogen product (GN2)

D. Crude Argon Column (CAC)

The configuration of CAC is shown in Fig. 6. The crude argon feed (CAR-F) comes from the middle tray of LPC, typically containing 89~91 wt% of oxygen. The purpose for FLASH is to separate the vapor and liquid crude argon, so FLASH is set at the same pressure as D2 and heat duty = 0. After exchanging heat with RL, the vapor phase of the crude argon (CAR-P) is sent to purified argon column (PAC) to purify. The liquid phase of the crude argon (R) becomes reflux of CAC. Because the heat exchanger (B13) is not at the equilibrium state, the pressure and temperature of RL (O2-EN-E) should be guessed.

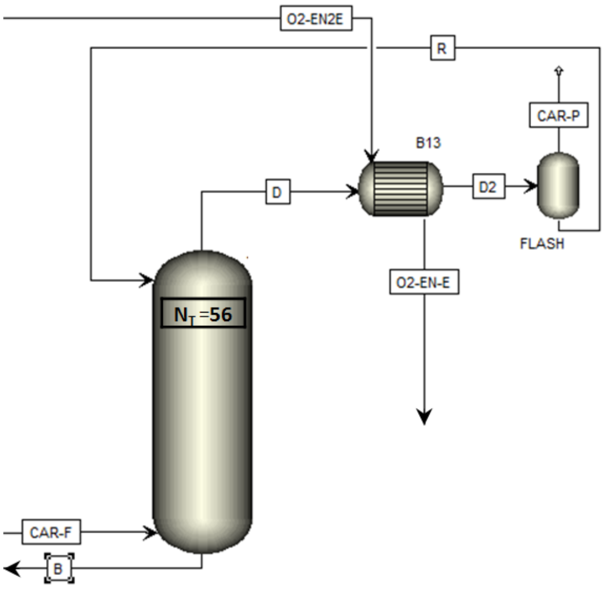

Fig. 6. The configuration of CAC

IV. FORMULA REGRESSION

To find out the formula among gaseous product demands and set point values, the range should include all the oxygen product demands. Six steady-state model is built to include all the oxygen product demands：17150 Nm3/h, 17600 Nm3/h, 17900 Nm3/h, 18350 Nm3/h, 18950 Nm3/h and 19100 Nm3/h. The formula can be built by using these steady-state models and plant data.

Refer to the ALC control, first, four product flowrates are set (these flowrates depend on product demands)：gaseous O_2 flowrate(GO2)、liquid O_2 flowrate(LO2)、gaseous N_2 flowrate(GN2_1)、liquid N_2 flowrate(LN2), and then calculate the state conditions which includes the crude argon flowrate and another gaseous nitrogen flowrate (this gaseous nitrogen is used as coolant for evaporation cooler outside the cold box).

State Calculation

Gaseous N_2 flowrate (GN2_2)

$$GN2\_2 = 3.2721 \times (GO2 + LO2) - 15998 - GN2\_1 \quad (1)$$

Crude Ar Flowrate (CAr)

$$CAr = 0.0384 \times (GO2 + LO2) - 170.78 \quad (2)$$

After having all the product flowrates, set point values can be calculated as follows.

Set Point Calculation

Air Flowrate (AirF)

$$\begin{aligned} AirF = [&(GO2 + LO2) \times 0.978 + 0.00191 \times CAr - (GN2\_1 + GN2\_2 \\ &+ LN2) \times 0.022] \div 0.188 \end{aligned} \quad (3)$$

HPC Reflux

$$HPC\,Reflux = 0.0014 \times GO2 + 53.887 \quad (4)$$

Rich Liquid (O2-EN)

$$O2\_EN = 1.6286 \times GO2 - 7677.9 \quad (5)$$

Waste N2 (WN2)

$$WN2 = AirF - GO2 - LO2 - CAr - GN2\_1 - GN2\_2 - LN2 \qquad (6)$$

Turbine Air Flowrate (TAir)

$$TAir = -0.0279x^2 + 28.331x + 5856.6 \qquad (7)$$
$$(x = LN2 \times 0.21 \div 0.78 + LO2)$$

Using these formulas, the operators can predict the final set points values while gaseous product demands change. But it needs the dynamic model to realize how to optimize the changing process.

V. CONTROL STRATEGY DEVELOPMENT

The overall control strategy is based on the actual control strategy of this ASU. Pressure-driven simulation in Aspen Plus Dynamics is used in the dynamics model. Some pressure drops and pressure values must be assumed due to the measurement error of pressure sensors and lack of some pressure data in the real plant. The holdups of all columns and flashers are calculated by the real plant design.

A. Inventory Control Loops

The control strategy in Aspen Plus Dynamics is shown in Fig. 7. The inventory and some simple regulatory control loops are determined first. In real plant, all the columns and some heat exchanges have levels control with level controllers by manipulating the bottom streams. Only LPC has the pressure control on the top of the column by manipulating gaseous nitrogen product. The other columns' pressure is related to the LPC's set point. In real plant, the crude argon feed flowrate is decided by the pressure difference between LPC and CAC. In real plant, the turbine air/air feed ratio is controlled by manipulating guide vane of the compressor, so there is a pressure controller (PC_TA) which controls the turbine air pressure. The temperature controller locates at the turbine air stream (TC_E02) is used to control the air temperature before entering cold box. In the real plant, the temperature is controlled by the cooling water flowrate, but this controller directly manipulates the heat duty in the simulation. The air feed, gaseous oxygen product and crude argon product are assigned as the throughput manipulator. All the control parameters are the same as the real plant setting.

B. Composition Control Loops

There are two composition controls in the real plant. One controls the oxygen composition in the HPC (CC_1), the other controls the oxygen composition in crude argon feed (CAF-F). The manipulated variable of the second controller is located at the gaseous oxygen product stream which outside the cold box and it does not in the simulation region. In real plant operation, all the composition control loops are in manual mode when load changes.

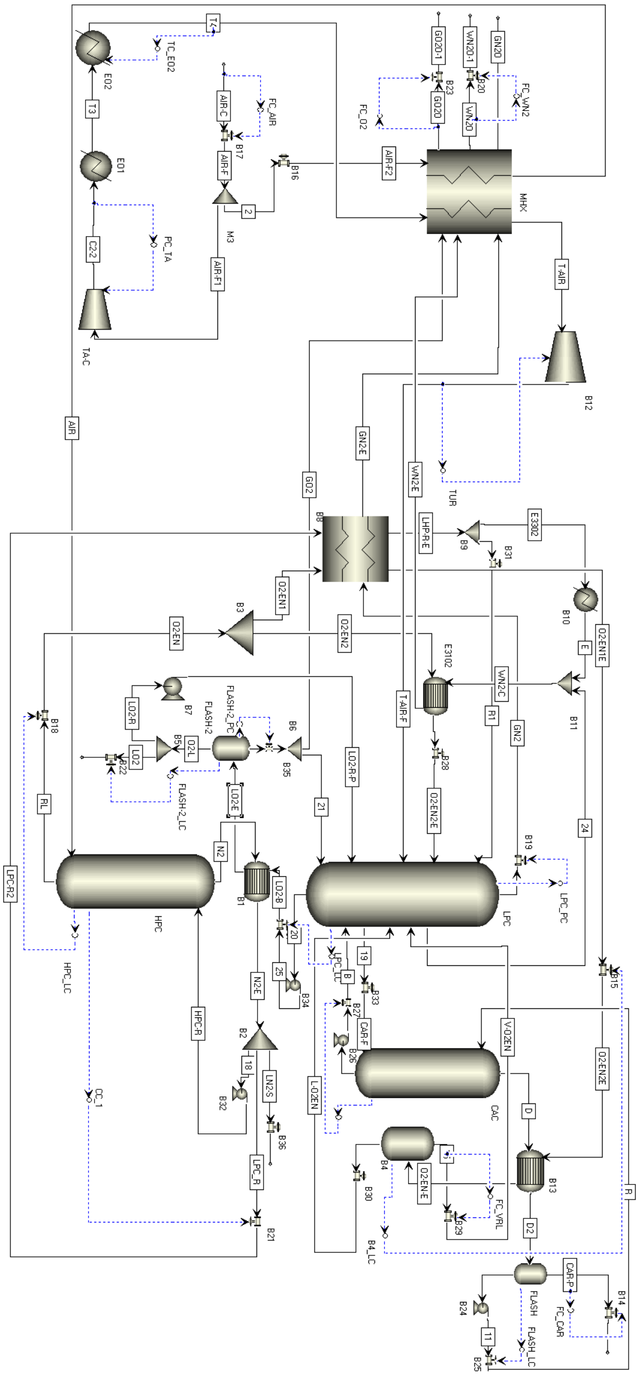

Fig. 7. Control strategy in Aspen Dynamics

C. Comparison between real plant data and simulation

One load change test is introduced to compare the accuracy of dynamic model with real plant data. The load change is based on the air throughput change. The air flow rate was decreased from 91000 Nm^3/h to 90000 Nm^3/h at about 9hr from the beginning of the test, and then increased to 91000 Nm3/h and 93000 Nm3/h at about 46hr and 50hr, respectively.

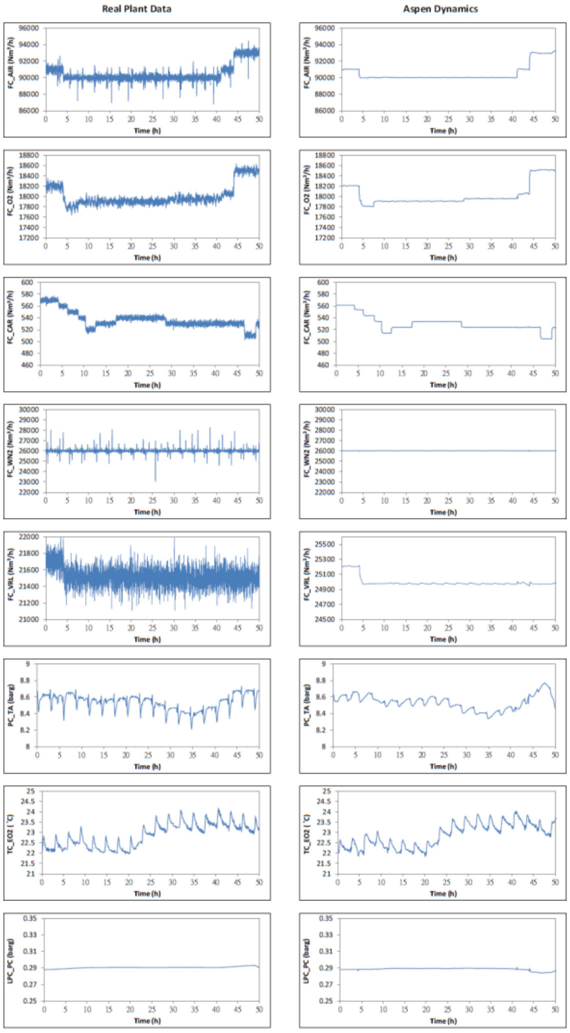

Fig. 8. Set points change

With the set point of air flowrate changes, the set points of oxygen flowrate (FC_O2), crude argon flowrate (FC_CAR), VRL flowrate (FC_VRL), waste nitrogen flowrate (FC_WN2), turbine air pressure (PC_TA), turbine air temperature (TC_E02), LPC pressure (LPC_PC) also changes to match the plant data. Fig. 8. displays the set points change of real plant data and simulation result.

The uncontrolled flow rates and compositions are shown in Fig. 9. Note that the dynamic trends of almost all variables are captured by dynamic model. The biggest difference between real plant data and simulation result is oxygen purity in the gaseous nitrogen product (GN2). There are two reasons might causing the large fluctuation between real plant data and simulation result. First, the oxygen purity is extremely low in the gaseous nitrogen product. Second, the fluctuation of turbine air pressure (PC_TA) and turbine air temperature (TC_E02) influence the feed enter the LPC.

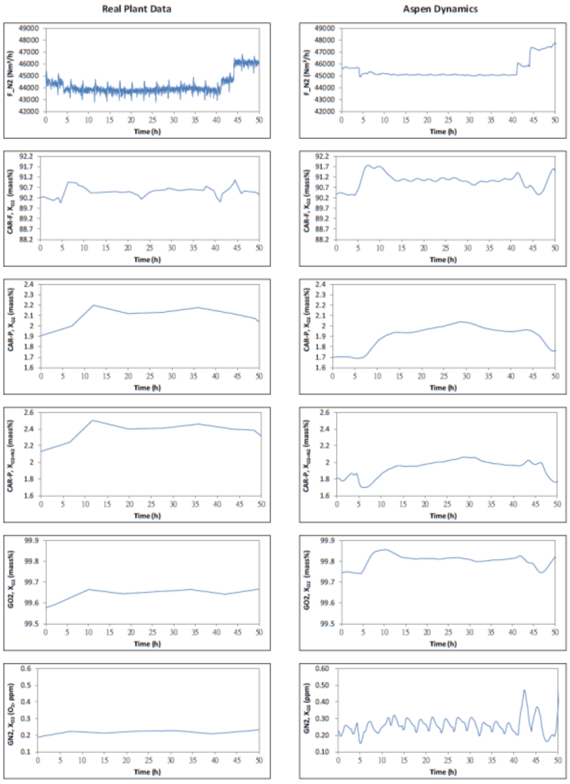

Fig. 9. Uncontrolled flowrates and compositions

VI. CONCLUSION

This paper demonstrates the steady-state and dynamic model of a real ASU, and find out the formula among gaseous product demands and set point values. In order to have the more accurate simulation results, PENG-ROB binary parameters have been adjusted. Using the adjusted parameters, the simulation results are much more close to the plant data.

As for the dynamic model, there are some differences between real plant data and simulation results due to the extremely low oxygen purity in the GN2 and the fluctuation of turbine air pressure and temperature. The improvement of the dynamic model to more closely fit the real plant data is still ongoing. After that, an automatic load change strategy will be developed for this air separation unit.

REFERENCES

[1] D. R. Vinson, "Air separation control technology," *Computers and Chemical Engineering*, vol. 30, pp. 1436-1446, 2006.

[2] S. Ivanova, R. Lewis, "Producing Nitrogen via Pressure Swing Adsorption," *Chemical Engineering Progress*, June 2012.

[3] Z. Xu, J. Zhao, X. Chen, Z. Shao, J. Qian, L. Zhu, Z. Zhou, H. Qin, "Automatic load change system of cryogenic air separation process," *Separation and Purification Technology*, vol. 81, pp. 451-465, 2011.

[4] R. Huang, V. M. Zavala, L. T. Biegler, "Advanced step nonlinear model predictive control for air separation units," *Journal of Process Control*, vol. 19, pp. 678-685, 2009.

[5] X. Liu, *Simulation, Optimization and Control of Distillation Processes (in Chinese)*, Beijing: Science Press, 2007, pp. 90-91.

[6] W. F. Castle, "Air Separation and Liquefaction: Recent Development and Prospects for the Beginning of the new Millennium," *International Journal of Refrigeration*, vol. 25, pp.158-172, 2002.